Thermoluminescence characteristics of the 375 °C electron trap in quartz

W. F. Hornyak
Physics Department, University of Maryland, College Park, Maryland 20742

Reuven Chen
School of Physics and Astronomy, Tel-Aviv University, Tel-Aviv, Israel 69978

Alan Franklin
Physics Department, University of Maryland, College Park, Maryland 20742
(Received 11 December 1991)

The thermoluminescence (TL) glow peak in quartz, which appears in the uv at a temperature of 375 °C when a ramp heating rate of 20 °C/s is used, was measured for emission in the uv as well as in the green part of the spectrum. Two glow peaks appear separated by about 20 °C. Isothermal decay rates for both spectral components were measured at temperatures near the glow peaks. Heating ramp rates were varied to obtain data for Hoogenstraaten analyses. Additive dose curves up to saturation were obtained. Solar-simulator bleaching studies were performed. Overall, these data appear to suggest a kinetic order between first and second order. It was found possible by computer simulation to reproduce faithfully the observed data by use of a simple interactive model that possesses two separate recombination centers, both simultaneously fed by electrons from a single electron trap and transported through the conduction band. It was found necessary to attribute a distribution of activation energies to the electron trap, to allow for a significant retrapping probability, and to also invoke the presence of a thermally disconnected electron trap. The analysis comparing the theoretical predictions to the data used a single set of program parameters in obtaining computer-generated solutions to 100 coupled differential-integral equations. These parameters successfully generated the observed initial rise values ranging from 0.9 to 1.1 eV (depending on the method employed) and an observed Hoogenstraaten-analysis energy of 1.49 eV both with a distribution central activation energy of 1.45 eV. A glow curve asymmetry shape factor $\mu=0.46$ given by the theory matched the data well, suggesting an apparent intermediate kinetic order. The theory also simultaneously generated the required uv-TL and green-TL glow peak separation in temperature. A model for generating the necessary electron and hole densities during laboratory additive dosing to reproduce the observed dose growth data was developed. This model is a consistent extension of the prior theoretical analyses. The electron activation energy distribution also provides a ready explanation for the midterm fading phenomenon present when radiation doses acquired during long burial times are compared to laboratory administered doses required to produce the same TL signal.

I. INTRODUCTION

The use of thermoluminescence (TL) as a dating tool has frequently relied on quartz as the principal dosimeter material. This is particularly so when employing the inclusion technique based on the use of selected grains of quartz in the 100–200 μm diameter range. When dating archaeological materials of considerable age, two high temperature and hence sufficiently stable glow peaks have been extensively used. These two peaks appear at 325 and 375 °C when using a heating ramp rate of 20 °C/s and when deep blue to near-ultraviolet (uv) transmission filters are employed with a quartz window photomultiplier. Only the 375 °C TL signal has been found to be "suitable" in its behavior when second glow results have to be correlated with those obtained from first glow measurements. The lower temperature signal has been found to be very unreliable under these circumstances.

Most recently, the lower temperature TL signal has become the subject of considerable interest in sediment dating because of its very rapid bleach when exposed to sunlight.[1–3] Not inappropriately, the 325 °C peak is referred to as the rapid-bleach peak (RBP) and the relatively slowly bleaching 375 °C peak is referred to as the slow-bleach peak (SBP). However even in sediment dating the 375 °C glow peak still retains considerable interest. This interest is in part due to the desire to be able to contrast dates derived from several techniques developed for the use of this 375 °C glow signal[4–8] with a number of methods that are based on using the rapid-bleach 325 °C signal, and are still being tested.[9–14]

We have undertaken an extensive experimental and theoretical investigation of the behavior of the 375 °C TL glow system because of its evident importance in dating methodology. An additional motivation is the understanding to be gained by such a study for the general underlying physics controlling charge trafficking in TL. In this respect, the seemingly simple glow system associated with the 375 °C peak exhibits many unexpected features making it an ideal case for general study.

II. EXPERIMENTAL ARRANGEMENT

The quartz material used in this experiment was from a relic sand dune of the Kalahari desert. Deposition of these dunes must have occurred more than 77 000 years ago.[15] The exposure to ionizing radiation over this time span was sufficient to lead to a very strong TL signal enabling a careful direct study of the "natural" material in its archaeological state. It is felt that this type of primary study would be the most relevant to dating technology.

The raw material used appeared to be very clean fine sand. This material was subjected to a chemical treatment consisting of exposure to: (a) 48% HF at 22 °C for 2 h with occasional stirring, (b) 3*N* HCl at 22 °C for 30 min, and (c) 30% H_2O_2 at 70 °C until bubbling stopped, approximately 10 h, and (d) repeated rinses in distilled water between these steps. This was followed by sieving to select grain sizes in the 90–120 μm range. Finally density separation was used to eliminate any heavy fraction present (i.e., density >2.70 g/cm^3). An x-ray-diffraction measurement failed to find in the final crystal clear material any mineral other than quartz.

In most cases the samples were directly deposited into a semispherical depression in a molybdenum heating strip. Holes were symmetrically drilled in the strip leading in either direction from this depression to reduce the temperature gradient in the sample containing area. Helium was used as the inert oven gas to surround the sample with a hot atmosphere. These efforts were taken to reduce the temperature difference between the sample and the thermocouple junction spot welded directly to the underside of the depression.

Glow curves were usually run at a ramp rate of 1 °C/s and never greater than 4 °C/s. All temperature measurements were monitored using a Fluke thermocouple thermometer directly incorporated into the oven control feedback system. The inherent precision of the Fluke thermometer is ±0.3 °C absolute. Glow curve temperature reproducibility was determined to be ±1.5 °C. Overall temperature determinations are believed to be better than ±2 K absolute. All data are weight normalized.

III. EXPERIMENTAL RESULTS

All present experiments were conducted under matched conditions employing in one case an ultraviolet filter (Schott UG11) in combination with an IR-absorbing Chance HA3 filter and in the other case a green filter (Chance O Gr 1) again in combination with a Chance HA3 filter; the former results are referred to as uv-TL results and the latter as green-TL results. The photomultiplier in each case was the same EMI 9635 Q tube. Using published quantum efficiency curves for this photomultiplier tube (PMT), the filter response functions, and the relevant wavelength range of the uv-TL and the green-TL emission, the detection efficiency for uv photons is estimated to be greater than for green photons by a factor of 8.3±2. These two filter arrangements are designed to separate the two TL emission peaks centered at wavelengths of approximately 380 and 480 nm,[3,16,17] respectively.

In order to isolate the desired 375 °C TL signal from the rapid-bleach 325 °C signal a 15 min exposure of the sample materials to green light was used. A further exposure of 15 min to green light produced no additional detectable difference in the resulting glow curves. This technique is identical to the one reported earlier regarding these two TL signals.[18]

A. Glow curve characteristics

Fairly well isolated glow curves in the uv and green are observed in the 250-450 °C range for the natural material prepared as described above. At a heating ramp rate of 1 °C/s the green-TL peak is at 331 °C (605 K) and the uv-TL peak is at 312 °C (585 K), about 19.5 °C lower. The peak TL emission rate is 2.19 times as large for the green photons uncorrected for detection efficiency. Figure 1 shows the glow curve shape of the average of six runs for the uv-TL compared to that of the average of ten runs for the green-TL. For this comparison the uv-TL results were temperature shifted by +19.5 °C and the TL yield multiplied by 2.19. Above about 370 °C the green-TL curves show the presence of higher temperature traps. The low-temperature side of the uv-TL curve shows some small peaks known to be strong in the uv and probably the result of phototransfer during the bleaching used to eliminate the RBP. In general the two SBP glow peaks are seen to be, in the main, very similar. The full width at half maximum (FWHM) intensity was 90.5° for both glow curves. The ratio of the upper temperature half width to the entire full width is $\mu=0.46$. This degree of asymmetry suggests an effective kinetic order between first order and second order, if shape modifications produced by the presence of any activation energy distributions that might be present are ignored. (In the context of the shape factor μ in Chen and Kirsh,[19] first-order behavior yields $\mu\approx0.42$, while second-order has $\mu\approx0.52$.)

Earlier results with this same natural material[2,18] showed that bleaching of the SBP with unfiltered solar-simulator light for periods up to 16 h produced an exponential decrease in green-TL yield with bleach time

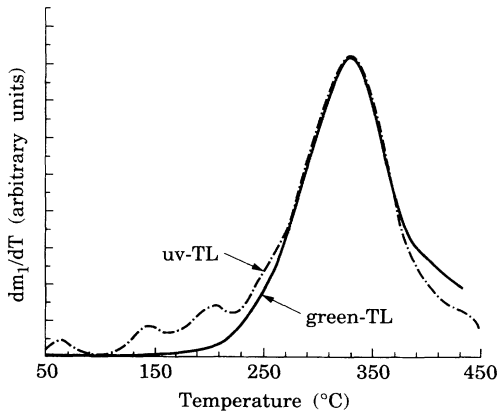

FIG. 1. Temperature shifted and height normalized superposition of the glow curves for the uv-TL and green-TL observed at a heating ramp rate of 1 °C/s.

down to a remanent steady rate 41% of the initial unbleached yield. During this bleaching process the glow peak gradually broadened, the breadth having increased by approximately 23% at the end of 16 h of bleach. In addition the glow peak gradually moved up in temperature with increased bleaching, shifting a total of 12.5° higher with 16 h of bleach. Both these behaviors also suggest a kinetic order higher than first order.

The effect of the heating rate on both the uv-TL and green-TL glow peaks was studied for the natural material at heating rates of 0.5, 1, 2, and 4 °C/s. From the lowest rate to the highest the two peaks shifted upwards by 42 °C, maintaining the separation of the peaks at about 20 °C. The results observed for the green-TL peak is shown in Fig. 2. In all cases the TL emission rate is per degree. When temperature shifted and normalized to the same peak height the glow peak shapes were essentially identical, maintaining a constant full width at half maximum of about 90°. The observed gradual decrease in peak height with increase heating rate thus appears to indicate a real loss of TL emission. The decrease from 0.5 to 4 °C/s of about 8% may well be due to thermal quenching.

Additive dose measurements were also performed on the same sand-dune material in the earlier investigation.[18] Laboratory γ-ray doses in steps of 50 Gy up to a dose of 250 Gy were administered to the natural material using a Co-60 source. In this instance the doses were calibrated to an absolute accuracy of ±3%. For convenience the glow growth curve obtained for the green-TL as a function of the added laboratory dose is reproduced as open circles in Fig. 3. A saturating exponential curve was found earlier to adequately match the data points.

The temperature of the glow peak maxima were found to decrease slightly with increasing dose. The total decrease with an added dose of 250 Gy was somewhat less than 10 °C. The temperature shifted and height normalized green-TL glow peaks are shown in Fig. 4. Except for slight shape changes on either side of the peak region the main glow structure appears to be essentially the same.

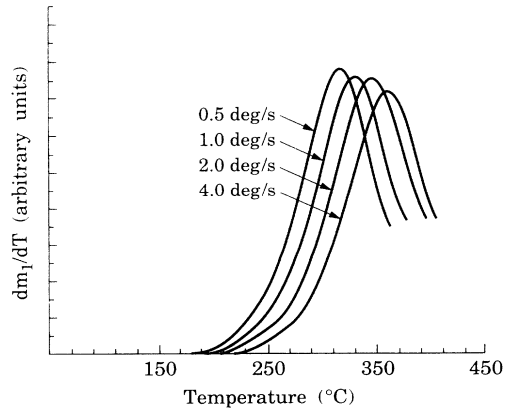

FIG. 2. Glow curve rates per degree (K) for green-TL as a function of the ramp heating rate from 0.5 to 4 °C/s. A TL-emission loss of 8% occurs from the beginning to the end of this range.

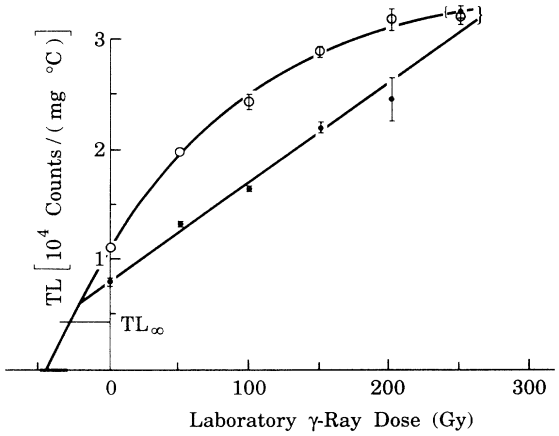

FIG. 3. First glow (open circles) and second glow (solid points) peak response growth curves for green-TL as a function of laboratory γ-ray dose, taken from an earlier result (Ref. 18). Solid-curved line is best fit by least squares of a saturating exponential and straight line is a linear regression fit. The ramp heating rate was 1 °C/s.

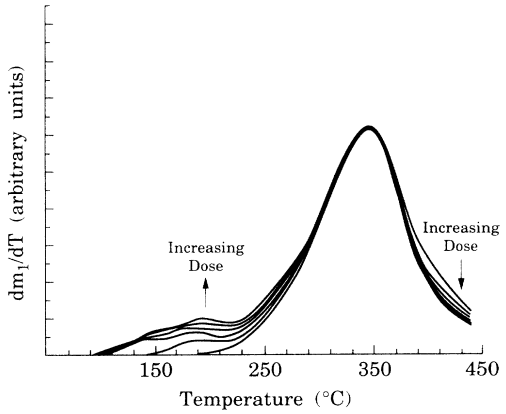

FIG. 4. Superposed temperature shifted and height normalized first glow curves for the additive dose data shown in Fig. 3. Except for dose related anomalies appearing to either side of the main peak the shapes are reasonably constant.

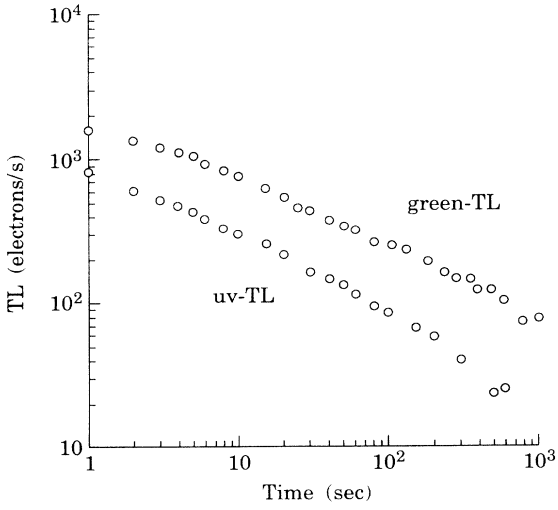

FIG. 5. Observed isothermal decay for green-TL and uv-TL at a temperature of 533 K.

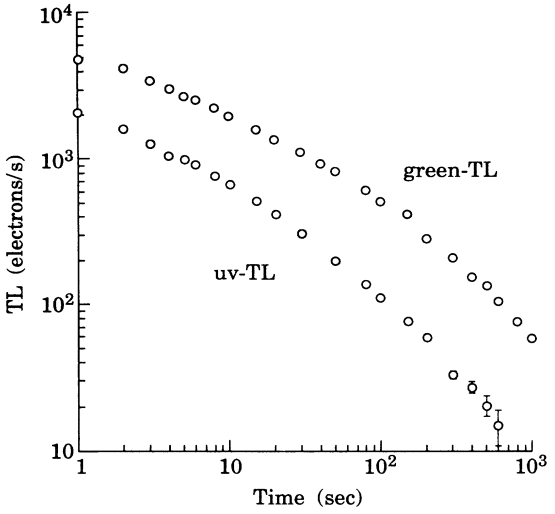

FIG. 6. Observed isothermal decay for green-TL and uv-TL at a temperature of 566 K.

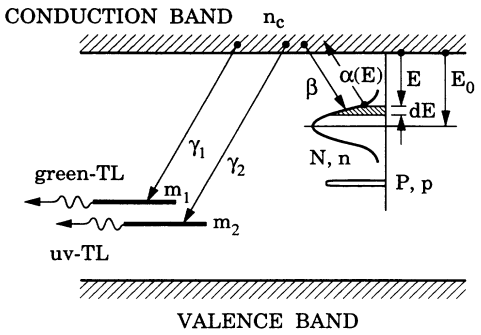

FIG. 7. A schematic representation of the charge trafficking giving rise to the observed TL emissions. A single active electron trap N possessing an activation energy distribution with central energy E_0, and two independent recombination centers interacting via the conduction band is assumed. A deep disconnected trap P is also taken into account.

Low-temperature structure, growing more rapidly with increasing dose than the SBP is also evident.

B. Isothermal characteristics

Isothermal decay curves were obtained for both the uv-TL and green-TL emissions of the natural material. Two separate temperatures were selected. The lower of the two, at 533 K was chosen to emphasize the early release of trapped charges with low activation energies if present, while the higher one at 566 K (just below the glow peak maxima) was chosen to emphasize the release of charges with possible higher activation energies.

Figures 5 and 6 show the results obtained. The uv-TL and green-TL decay curves at each temperature appear to differ mostly by a multiplicative constant. The decay curves are distinctly nonexponential in their variations with time; rather they appear more nearly to obey power laws. For example, at 533 K the decay curves are approximately of the form $t^{-\nu}$ with $\nu=0.45$ for the green-TL and $\nu=0.54$ for the uv-TL.

IV. DATA ANALYSIS

An attempt is made in the following to fit the data with numerical calculations based on a simple set of theoretical assumptions involving the least number of parameters possible. While as might be expected, a precise fit to all the measured results is not possible, the model developed does reproduce the general behavior well and produces a good fit to much of the critical data.

A. Theory

The assumption is made that electrons thermally elevated from traps are transported through the conduction band to recombination centers. Figure 7 is a schematic representation of the assumed charge trafficking giving rise to the observed TL emissions.

Central in this analysis is the presence of two glow peaks separated by 20 °C in temperature and emitting in the green and in the uv, respectively. The immediate hasty conclusion that therefore two electron traps must be present does not necessarily follow, especially if the similarity in shape of the two glow curves is noted (Fig. 1). In the following, it will be demonstrated that a single electron trap center feeding two independent recombination centers can in fact produce two temperature separated glow curves when the light characteristic of the two centers is viewed with appropriate transmission filters. This phenomenon is a particularly simple version of interactive kinetics that generally embodies the coupling of several distinct electron and hole densities through electron trafficking in the conduction band. The possibility for such behavior has been suggested earlier by Bonfiglioli *et al.*[20]

Conforming to this model, only a single thermally active type of electron trap is assumed having a total concentration N with n electrons present at any particular time. To allow for a possible distribution of activation energies E, a Gaussian distribution function $\rho(E)$ is assumed:

$$\rho(E)=N\sqrt{a/\pi}\exp[-a(E-E_0)^2] \tag{1}$$

and

$$\int_0^\infty \rho(E)dE=N\ . \tag{1a}$$

In a manner similar to that adopted in an earlier study[21] an electron occupation number $f(E,t)$ is adopted such that an electron distribution $\eta(E,t)$ may be written

$$\eta(E,t)=f(E,t)\rho(E) \tag{2}$$

and

$$n=\int_0^\infty f(E,t)\rho(E)dE\ . \tag{2a}$$

It is assumed that the beginning of every TL process, i.e., at $t=0$ or $T=T_0$, we have

$$\eta(E,0)=f_0\rho(E) \tag{2b}$$

with f_0 a constant; that is, the original electron distribution is also Gaussian. The thermal release of electrons is taken to be governed by an Arrhenius probability per electron, $\alpha(E)=se^{-E/kt}$ where the frequency factor s is assumed to be energy and temperature independent. The number of trapped holes in the two recombination centers at any time are designated m_1 (for the green-TL center) and m_2 (for the uv-TL center). The number of electrons in the conduction band is labeled n_c. A temperature- and energy-independent retrapping factor β, and recombination transition probabilities γ_1 and γ_2 are assumed.

A possibility of a deep thermally disconnected electron trap with concentration P occupied by p electrons is also assumed. The activation energy for this trap is assumed to be large enough to prevent its participation in the various TL processes. Recall that we are treating sand-dune material that has probably not been at an elevated temperature for a long geological period. It is assumed that during this time continual exposure to natural ionizing radiation resulted in this trap being saturated, i.e., $p=P$, so that no further trapping from the conduction band need be considered.

Finally, the governing charge trafficking integral-differential equations are

$$\begin{aligned}\frac{d\eta(E,t)}{dt}dE&=\rho(E)\frac{df(E,t)}{dt}dE\\&=-\alpha(E)\rho(E)f(E,t)dE\\&\quad+\beta[1-f(E,t)]\rho(E)n_c dE\end{aligned} \tag{3a}$$

and, of course, in view of Eq. (2a),

$$n(t)=\int_0^\infty \eta(E,t)dE\ , \tag{3b}$$

$$\begin{aligned}\frac{dn_c}{dt}&=\int_0^\infty \alpha(E)\rho(E)f(E,t)dE\\&\quad-\beta n_c\int_0^\infty[1-f(E,t)]\rho(E)dE\\&\quad-\gamma_1 m_1 n_c-\gamma_2 m_2 n_c\ ,\end{aligned} \tag{4}$$

$$\frac{dm_1}{dt}=-\gamma_1 n_c m_1\ , \tag{5}$$

$$\frac{dm_2}{dt}=-\gamma_2 n_c m_2\ , \tag{6}$$

and at all times

$$n+n_c+p=m_1+m_2\ . \tag{7}$$

To allow for one overall intensity normalization that would include detection efficiency factors etc., the value of N is not specified. If Eqs. (3)–(7) are all divided by N, then we more conveniently deal with relative concentrations and TL rates: n/N, m_1/N, . . . , $d(n/N)/dt$, $d(m_1/N)/dt$, . . . and transition rates βN, $\gamma_1 N$, etc.

The method used to solve Eqs. (3)–(7) was to subdivide the Gaussian distribution of N, $\rho(E)$, into 96 separate equal narrow sections. The electron population in each section was treated independently, each with its own release parameter $\alpha(E)$ and with a common retrapping parameter β. In addition to these equations embodied in Eq. (3a) the other four conditions Eqs. (4)–(7) were also programmed and numerically solved by using a subroutine based on the sixth-order predictor-corrector Runge-Kutta method. Tests varying the number of sections into which N was subdivided showed no significant change in the results in using more than the 96 sections adopted.

As time or temperature increases the distribution of electrons that first started out Gaussian in shape gradually becomes asymmetric, generally favoring the deeper traps. This results from the fact that the electrons with the lowest activation energy are released earliest, while the retrapping probability is independent of energy, so that occupation of the deeper traps may actually be enhanced by retrapping.

An important feature contained in the bimolecular interactive form of Eqs. (5) and (6) leads to

$$\frac{d}{dt}\left[\frac{m_1}{m_2}\right]=(\gamma_1-\gamma_2)\left[\frac{m_1}{m_2}\right]n_c\ . \tag{8}$$

It follows that

$$\frac{dm_1/dt}{dm_2/dt}=\frac{\gamma_1 m_{10}}{\gamma_2 m_{20}}\exp\left[(\gamma_1-\gamma_2)\int_0^t n_c(t)dt\right]\ . \tag{9}$$

Thus, unless $\gamma_1=\gamma_2$, the ratio of the TL in the two emission bands will vary with time (or temperature) in a complicated manner. The actual behavior is quite different from that expected if only a simple branching ratio modification of a TL-release expression is used for whatever kinetic order. Such a simple approach is clearly not valid.

B. Data fitting

We note that applying Eqs. (3)–(7) requires the selection of what at first glance appears to be a large number of independent parameters: initial values n_0, m_{10}, m_{20}, p; decay constants γ_1, γ_2, β; TL release constants s, E_0 and width parameter a appearing in the Gaussian activation energy distribution. Although all of these parameters interact in complicated ways when any particular data set is examined in terms of these integral-differential equations, a number of conditions or critical clues can from the outset reduce the ambiguities present.

1. The parameters γ_1/γ_2, n_0, m_{01}, m_{02}, and p

Referring to Eqs. (5) and (6), we note that we have for the logarithmic derivatives

$$\frac{1}{m_1}\frac{dm_1}{dt}\Big/\frac{1}{m_2}\frac{dm_2}{dt}=\frac{\gamma_1}{\gamma_2}\ . \tag{10}$$

These logarithmic derivatives may be directly related to the observed TL and the respectively "light sums," e.g., $\int_t^\infty (\mathrm{TL})dt$. Detection efficiencies, weight normalization, etc., cancel out in this equation as does the common value of n_c.

First we examine the result of applying Eq. (10) to the glow curves for green-TL and uv-TL. Figure 8(a) shows that when light sums are used to define m_1 and m_2 the ratio γ_1/γ_2 does not appear to be constant, contrary to the assumptions. However, if a particular constant value (60% of m_{01}) is added to the light sum defining m_1 it is possible to obtain a constant value 0.32 for γ_1/γ_2 [Fig. 8(b)]. We assume that this constant additive value arises from the hole counterpart to the deep disconnected electron trap P and is equal to the saturated value p. The success of this simple assumption may be judged by the fact that the curves in Figs. 8(a) and 8(b) extend well over the glow curve peaks and to a point where the green-TL light sum is less than 50% of its initial value.

Applying Eq. (10) to the 566 K isothermal data for the green-TL and the uv-TL leads to results for the ratio of γ_1/γ_2 shown in Figs. 9(a) and 9(b). Again when the *same* percentage increase in m_{01} is assumed as required in adjusting the data of Figs. 8(a) and 8(b) the ratio γ_1/γ_2 is seen to become a constant 0.34 very close to the value obtained from the glow curves. Again note that the data extends to a point where the green-TL remanent light sum is less than 30% of its initial value.

The data for the 533 K isothermal experiment when treated the same way yields a constant value for $\gamma_1/\gamma_2=0.42$. In this case the data points do not extend to as large a reduction in remanent light sum. In view of these results we assume an average value of 0.36 for the ratio of the parameters γ_1 and γ_2. Since the uv-TL glow peak is at a lower temperature than is the green-TL glow peak we must have $\gamma_2 > \gamma_1$.

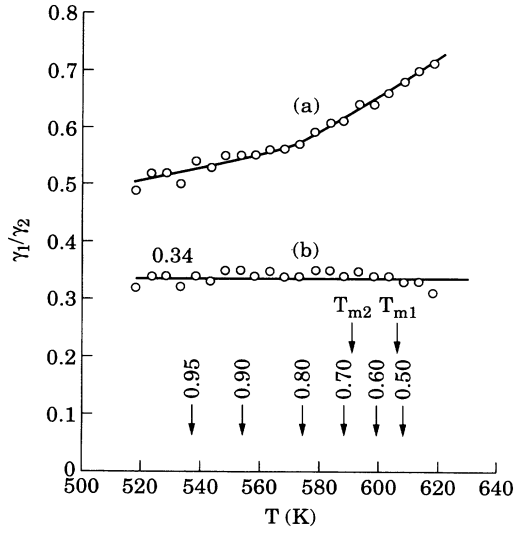

FIG. 8. (a) Experimentally determined ratio γ_1/γ_2 from the green-TL and uv-TL glow curves taken at a heating ramp rate of 1 °C/s, see Eq. (10) of text. The data points assume m_1 and m_2 proportional to the respective "light sums." (b) Same calculation when the instantaneous value of m_1 is increased by a constant value (60% of m_{01}) assumed to be associated with a saturated disconnected trap P. The bottom range of numbers indicate the remnant light sum in the green-TL as a fraction of the initial amount present. The location T_{m1} and T_{m2} of the two glow peaks is also indicated.

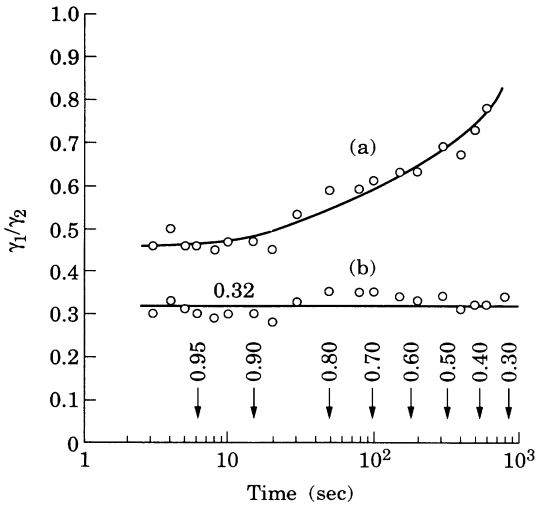

FIG. 9. (a) Experimentally determined ratio γ_1/γ_2 from the green-TL and uv-TL isothermal decay curves taken at a temperature of 566 K, see Eq. (10) of text. The data points assume m_1 and m_2 proportional to the respective "light sums." (b) Same calculation when the value of m_1 is increased by the same constant value used to generate Fig. 8(b). The bottom range of numbers indicate the remnant light sum in the green-TL as a fraction of the initial amount present.

If the saturating behavior of the dose curve shown in Fig. 3 is attributed to saturation of the electron trap population n, we may assume for the natural (undosed) sample that $n_0/N=0.330$. Noting the required additive constant to the light sum of m_1 necessary to yield a constant ratio of γ_1/γ_2, the small value needed for $m_{02}/N=0.017$ to produce the proper observed ratio of the green-TL glow peak height to that of the uv-TL glow peak, and the constraint of Eq. (7), we arrive at the initial, i.e., $t=0$ (or $T=T_0$) values:

$$\begin{aligned} n_0/N &= 0.330\ , \\ m_{01}/N &= 0.510\ , \\ m_{02}/N &= 0.017\ , \\ p/N &= 0.197\ . \end{aligned} \tag{11}$$

To isolate the uv-TL glow peak required a brief preliminary bleaching with a green or yellow filter to remove the interfering RBP signal. Experiments on this bleaching process showed that it had no impact on the glow peak of either the uv- or the green-TL signal of the SBP. These observations were taken to indicate that neither m_1, m_2, nor n were affected by this bleach.

2. *The energy release parameters s, E_0, and a*

Ample evidence exists in the literature that the initial rise method[19,22] for obtaining the values of s and E will not yield physically correct results.[23–26] However, it is instructive to treat the green-TL glow curve data ob-

tained at a heating rate b of 1 °C/s as if it were the *only known data.* The results obtained with versions of the initial rise analysis of this data will again lead to unacceptable values for s and E.

If the TL behavior is strictly first order, so that

$$-b\frac{dm}{dT}=sme^{-E/kT} \tag{12}$$

is assumed a plot of

$$\ln\left[-\frac{1}{m}\frac{dm}{dT}\right],$$

as a function of $1/T$ should yield a straight line graph with a slope of $-E/k$ and a y intercept of $\ln s/b$. Figure 10 (open circles) shows a plot of this type for the data; the values of m are derived from the unaugmented light sum. The initial rise portion of the curve to a temperature yielding about $\frac{1}{4}$ maximum TL rate yields $E=0.91$ eV. However at higher temperatures the data points deviate considerably from the predicted straight-line behavior.

If instead of Eq. (12) the modified form known as the general order theory (GOT) equation:[27]

$$-b\frac{dm}{dT}\left[1+\frac{\beta N}{\gamma m}\right]=mse^{-E/kT} \tag{13}$$

is used, the fit shown in Fig. 10 (with solid points) results. The fit now is remarkably accurate, well over the glow

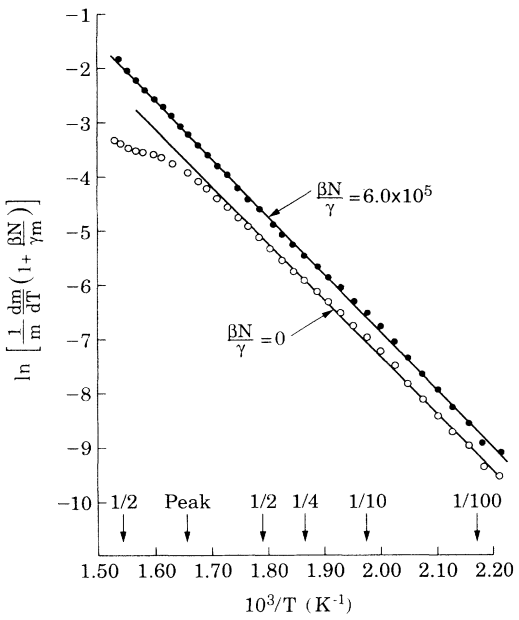

FIG. 10. The function

$$\ln\left[\frac{1}{m}\frac{dm}{dT}(1+\beta N/\gamma m)\right] \text{ vs } 1/T$$

for the green-TL glow curve at a ramp heating rate of 1 °C/s. The curve with the open circles is for a strict first-order behavior with $\beta N/\gamma=0$ and the curve with solid points is for the so-called GOT equation fit with $\beta N/\gamma=6.0\times10^5$.

curve peak down to a point where the interference of a higher temperature trap becomes significant. The value of E is now 0.92 eV, virtually the same as for the first-order fit. The value of s is found to be 1.8×10^6/s. The parameter combination $\beta N/\gamma=6.0\times10^5$ results and is not further reducible into its component parts without additional data.

The excellent fit obtained by use of the GOT equation yields parameters that nonetheless fail to predict the observed glow peak temperature shift with heating rate. In addition when the same analysis is applied to the green-TL glow curve at a heating rate of 4 °C/s the value of E turns out to be 1.02 eV. The isothermal decay data at both 533 and 566 K are very badly fitted by this theory, yielding only slightly modified exponentials. Of course it also leaves the uv-TL results totally uncoupled. This situation should again be a warning about the chameleon-like behavior of glow curve data when viewed isolated from other TL measurements.[21]

The most striking failure of an approach involving equations such as Eqs. (12) and (13) or their differential equation versions is the total failure to reproduce the shape of the isothermal decay curves. Only by introducing an activation energy distribution is it possible to obtain an approximation to the power-law behavior with time indicated by the data. Returning to Eqs. (3)–(7), we note that for the early times when n, m_1, and m_2 are essentially their initial values n_0, m_{01}, and m_{02}, the imposition of the Gaussian (or any other) distribution of E simply adds a multiplicative modifying function to the decay function that would result with no distribution. For the Gaussian distribution of Eq. (1) this multiplicative function is

$$\frac{yG(x,y)}{\sqrt{\pi}}, \tag{14}$$

where

$$x=\alpha_0 t,\ \alpha_0=se^{(-E_0/kT)},\ \text{and } y=kT\sqrt{a}\ .$$

The function $G(x,y)$ is the "after effect" function[21,28,29] and is identical to $f(x,y)$ of Jahnke and Emde[30] where it appears in a tabular format as well as in a graphical presentation. Examining the behavior of $G(x,y)$ for times less than 10 sec at $T=533$ K rapidly establishes that $\tau_0=1/\alpha_0$ must be in the range 50 to 200 sec and that $60<a<100$ (eV)$^{-2}$.

The peak temperature T_m and the width ω of the glow curve peak also constrains the value of E_0. With other parameters held fixed E_0 increases with T_m approximately proportional to T_m^2/ω (see Chen and Kirsh[19]).

A further constraint on E_0 is the requirement imposed by the glow curve peak temperature T_m shift with heating rate b. In the absence of a distribution of activation energies the slope of the plot of $\ln(T_m^2/b)$ vs $1/T_m$, the so-called Hoogenstraaten plot, should yield the value E_0/k.[31] To the extent that the glow curve behavior can be characterized by Eq. (13), this should be a very good approximation regardless of the value of β (i.e., the "order" of the process). The actual data plotted this way suggests a value of $E_0=1.49$ eV. Since the addition of an

activation energy distribution might lower the required value of E_0 to achieve this result, it is reasonable to conclude from this and the initial rise analysis that $0.92 < E_0 < 1.49$ eV, with E_0 more likely to lie near the upper end of this range. Final values selected to give the best overall fit to the data are $E_0 = 1.450$ eV, $a = 80$ $(\text{eV})^{-2}$, and $s = 5.1 \times 10^{11}\ \text{s}^{-1}$.

3. *The parameters γ_1, γ_2, and β*

The parameters γ_1, γ_2, and β have the effect of shifting the temperature of the glow peak maxima. Decreasing either γ_1 or γ_2 largely only increases the temperature of the corresponding glow peak maximum, while increasing β increases the peak positions for both TL emissions simultaneously. These effects are present for all activation energy distributions, including $a = \infty$. However, decreasing a alone has the effect of shifting both glow peak maxima to higher temperatures.

As discussed above the ratio γ_1/γ_2 is fixed rather directly by the data, leaving the difference $\gamma_2 - \gamma_1$ still to be determined, mainly from the difference in the peak temperatures of the uv- and green-TL glow curves.

The factorization discussed in connection with Eq. (14) during the earliest phase of isothermal decay (near $t = 0$) that treats n, m_1, and m_2 constant at their initial values shows that n_c and hence dm_1/dt are close to saturating exponentials. The decay rate constant of this exponential is readily found using Eqs. (3)–(7) to be

$$\beta(N - n_0) + \gamma_1 m_{01} + \gamma_2 m_{02}\ s^{-1} . \tag{15a}$$

Since the experimental isothermal decay curves do not show any further rising portion just after the samples reach thermal equilibrium, it may be concluded that this feature of the initial behavior is mostly over. Using the values adopted for γ_1/γ_2 and the initial values given in Eq. (11) it follows that

$$0.67N\beta + 0.56\gamma_1 N \geq 1 s^{-1} . \tag{15b}$$

This condition further limits the possible choices for $N\beta$ and $N\gamma_1$.

Taking all these effects into account the best values for the bimolecular rate parameters are

$$\begin{aligned} N\beta &= 3.5 , \\ N\gamma_1 &= 1.3 , \\ N\gamma_2 &= 3.5 . \end{aligned} \tag{16}$$

V. FINAL THEORETICAL FIT

Not all the experimental results could be fitted with great precision using the parameters quoted in Sec. IV. To begin with, the model did not allow for any thermal quenching and hence the total TL emissions at the various heating rates were held constant contrary to the actual data.

The parameters finally selected were the values that yielded the best overall fit to the designated high priority features of the green-TL and uv-TL results.

A. Glow curves

Figure 11 shows the experimental data points for the green-TL glow curve (open circles) at a 1 °C/s heating rate and the theoretically derived curve. The points (open diamonds) and the corresponding theoretical curve for the uv-TL glow curve are also shown in Fig. 11. Both simultaneous theoretical curves result from a single normalization $N = 1.05 \times 10^6$, in units relevant to actual detected counts. This value corresponds to an actual electron trap density of the order of $10^{14}/\text{cm}^3$. The agreement on the glow maxima follows from the selection of m_{02}/m_{01} and the efficiency ratio of 8.3 for detecting the uv-TL relative to the green-TL. If the efficiency ratio were unity the green-TL maximum rate would be 18.3 times as large as the uv-TL maximum rate.

Not only are the full widths $\omega_1 = \omega_2 = 90.5$ °C reproduced but the correct shape parameters $\mu_1 = \mu_2 = 0.46$ are also obtained. Finally, the peak temperature difference between the two curves of 19.5 °C is also accounted for.

The close agreement between the theory and the data suggests that in both cases the initial rise plot of ln $(-dm_1/dT)$ vs $1/T$ should also yield the same slope and apparent value for an effective E. Indeed the theoretical value arrived at is 0.95 eV, close to the data derived value of 0.92 eV. It is to be noted that these values are very much lower than the $E_0 = 1.450$ eV used in the theory. This result is in agreement with an earlier finding that showed that with a distribution of activation energies the initial rise effective value of E emphasizing as it does the

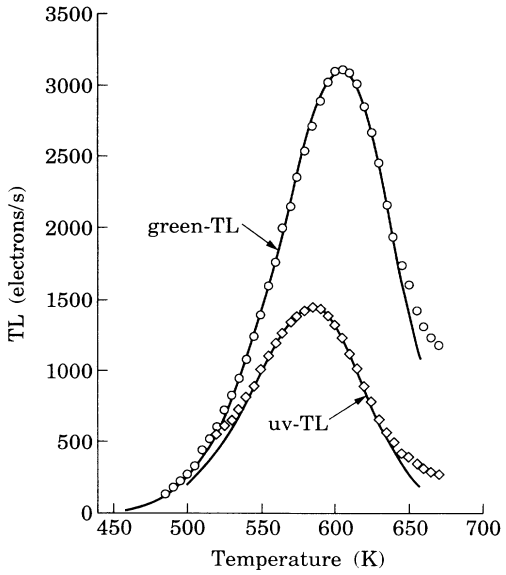

FIG. 11. (a) The experimental data points (open circles) for the green-TL glow curve at a ramp heating rate of 1 °C/s. The curve is the theoretical fit. (b) The experimental data points (open diamonds) for the uv-TL glow curve at the same ramp heating rate. The curve is the simultaneous theoretical fit with no temperature shift or extra height renormalization employed. In both cases the curves are averages over many weight normalized aliquot samples.

initial release of the least bound electrons, will always be lower than the actual mean value of the distribution.[21,32]

B. Heating rate effects

The green-TL glow curves were run at heating rates of $b=0.5$, 1, 2, and 4 °C/s. The theoretical parameters used for the 1 °C/s fit were used to calculate the glow curves at the other heating rates. The agreement between the calculated values of the temperature T_m at the glow curve maximum and the observed values was very good.

As remarked earlier, plotting ln (T_m^2/b) vs $1/T_m$ should also give an effective activation energy from the slope of the resulting curve. The data points and the theoretically derived points, and a straight line drawn through the latter for this method of defining E are shown in Fig. 12. The error flags on the data points correspond to an estimate of ±2° K absolute. The slope of this straight-line fit yields $E=1.49$ eV, only slightly higher than the value of $E_0=1.45$ eV used in the theory. Such a discrepancy is to be expected because of the distorting effect retrapping has on the electron distribution in activation energy as the glow peak develops. In this process the mean electron activation energy is shifted upwards.

Although no data was taken at a heating rate of 20 °C/s, the theoretical value for T_m for the uv-TL glow curve was calculated. It was predicted to be 378 °C close to the literature value of 375 °C.

Somewhat less satisfactory was the theoretical prediction of glow curve widths ω as the heating rate is varied. The calculated width slowly increases with heating rate. For example, at a heating rate of 4 °C/s the width of the green-TL glow curve should increase to $\omega_1=105$ °C whereas the experimental value remains about 91 °C, the same value for all the heating rates. Since the theory assumed that the total TL yield was a constant the glow peak height slowly decreased as the width increased keeping the product (and hence the glow area) a constant.

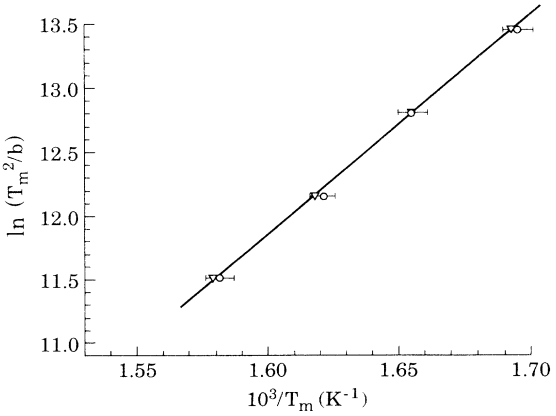

FIG. 12. The Hoogenstraaten-analysis plot of $\ln(T_m^2/b)$ as a function of $1/T_m$ for ramp heating rates of 0.5, 1, 2, and 4 °C/s. The open circles with the associated "error flags" are for the experimental data. The triangles are the corresponding theoretical points. The straight line drawn through the latter points yields a slope corresponding to an effective $E_0=1.49$ eV.

C. Isothermal studies

Figure 13 shows the experimental data points (also shown in Fig. 5) as well as the calculated theoretical curves for the isothermal decay at 533 K. To have the theoretical curves pass through the data points required the slight intensity renormalization of both the green-TL and uv-TL calculations. Figure 14 shows similar results for the isothermal decay at $T=566$ K. Once again slight intensity renormalizations were required.

For each spectral TL-type theoretical results are shown for δ-function narrow activation energy distributions, using the same parameters but with $a=\infty$. The resulting shapes are basically modified exponentials. No amount of varying the parameters could produce the necessary power-law-type shapes.

The isothermal decay with time of the trapped charge concentrations of a simple TL system involving a single electron trap and a single recombination center with no retrapping but with a Gaussian activation energy distribution is essentially controlled by the function $G(x,y)$ cited in Eq. (14).[21] For temperatures sufficiently close to each other for the shape parameter $y=kT\sqrt{a}$ to be sensibly the same the concentration of trapped holes (or electrons) vs $x=\alpha_0 t$ would fall on the same "universal" curve regardless of temperature. Since TL is proportional to $-dm/dt$, TL/α_0 plots would also form a universal curve.

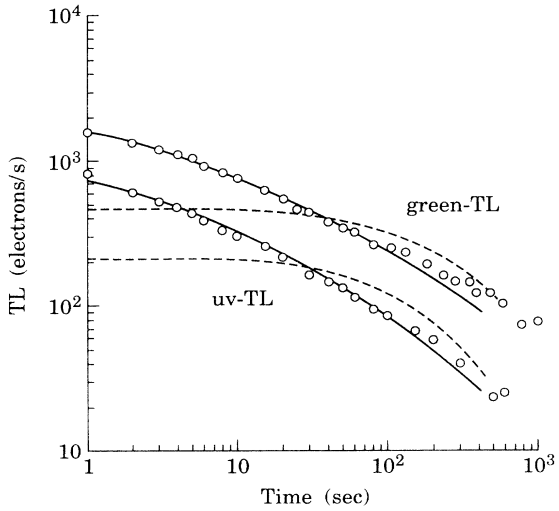

FIG. 13. Green-TL and uv-TL experimental isothermal decay data (open circles) at a temperature of 533 K. The solid curves are the theoretical fits using the same parameters as those used in Figs. 10–12. In each case the data are for single aliquot runs, hence a small renormalization in height (of the order usually observed run-to-run) was applied in each case to give the best match to the data for $t<50$ s. The dashed curves are for the same theoretic parameters and normalization but with a δ-function width for the activation energy distribution in place of the adopted Gaussian distribution.

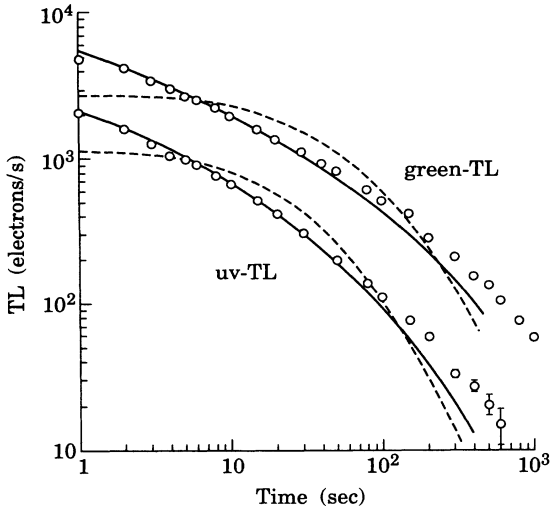

FIG. 14. Green-TL and uv-TL experimental isothermal decay data (open circles) at a temperature of 566 K. The solid curves are the theoretical fits using the same parameters as in Figs. 10–13. A slight height renormalization of the theory was required for each curve to best match the data for $t < 50$ s in order to allow for possible aliquot-to-aliquot variations.

To test if the same type of universal plot pertains to the case in hand, which includes both retrapping and interactive kinetics generated by the presence of two recombination centers, the data and the computer generated theoretical results at $T = 533$ and 566 K were replotted as functions of x and yield normalized by the ratio of α_0 at the two temperatures. The results are shown in Fig. 15. To a remarkable extent a single plot emerges.

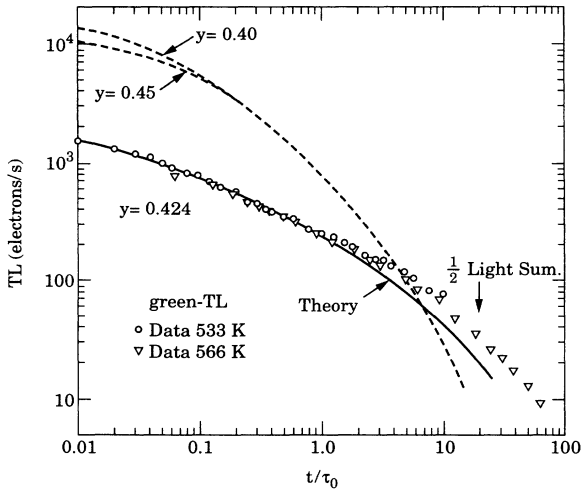

FIG. 15. The universal plot for the green-TL data shown in Figs. 13 and 14 resulting from converting the time variable t to $x = \alpha_0 t$ and normalizing the yield through the factor α_0. The data light sum is reduced to $\frac{1}{2}$ its initial (i.e., $x = 0$) value at both temperatures when $x = 20$ in each case. The after effect function $G(x,y)$ is also shown, the values of y indicate the range spanned in the isothermal experiments.

Figure 15 also exhibits the function $G(x,y)$ for values of y corresponding to both $T = 533$ and 566 K, shifted vertically to avoid confusion. The point made earlier should be noted, that for small values of x, $G(x,y)$ and the actual data track well to within a multiplicative constant. The effect of retrapping in retarding electron release to later times is evident in comparing $G(x,y)$ to the actual data.

Figure 13, 14, and 15 are the most convincing evidence for the need to introduce both a distribution of activation energies for the trapped electrons as well as a significant retrapping process.

D. Dose-related effects

Figure 3 shows the rapidly saturating behavior of the green-TL glow yield as the laboratory additive dose is increased. In the parameter evaluations this was attributed to the saturation of the number of electrons n that can occupy the total number of available sites N. Since the TL yield is not directly associated with n it remains to be shown that this assumption is reasonable.

To test this hypothesis a dose-responsive trap-filling model was adopted, both consistent with the TL model of Fig. 7 and permitting the same values of the parameters to be used in common. This model has been explored by Chen, McKeever, and Durrani in another context.[33] This trap-filling model is shown in Fig. 16 where the necessary new parameters M_1, M_2, λ_1, and λ_2, are introduced along with a new variable h to represent the number of holes present in the valence band at any time. It is assumed that the laboratory dosing is at ambient temperature for relatively short periods of time and hence the release parameter $\alpha(E,T)$ may be taken equal to 0. Since the trapping parameter β in the earlier model was taken to be energy independent there is no need in the present model under the same assumption to exhibit the activation energy distribution, which, of course, is still present. Consistent with an earlier assumption it is assumed that the deep electron trap P is saturated throughout, i.e., $p = P$,

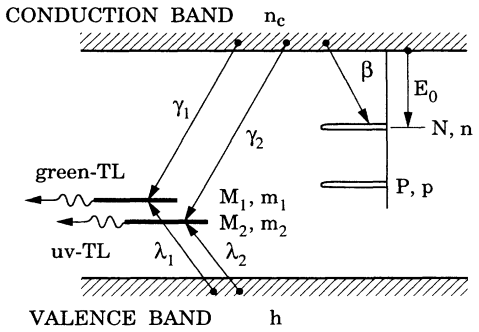

FIG. 16. A schematic representation of the charge trafficking occurring during the additive dose process. The γ-ray dose is applied at room temperature leading to considerable simplification in the number of necessary parameters. Trap filling is assumed to proceed through electron and hole production in the conduction and valence bands.

and therefore no trapping parameter involving P is necessary. A constant rate of dosing R is assumed to act for a time Δ yielding a total dose D, i.e., $D=R\Delta$. After the dose D has been administered the subsequent relaxation of both n_c and h must be allowed for. A numeric computational program to arrive at the values for n, m_1, and m_2 resulting from this dosing process was written. The relevant differential equations solved are

$$\frac{dn}{dt}=\beta n_c(N-n)\ , \tag{17}$$

$$\frac{dn_c}{dt}=R-\beta n_c(N-n)-\gamma_1 n_c m_1-\gamma_2 n_c m_2\ , \tag{18}$$

$$\frac{dm_1}{dt}=\lambda_1 h(M_1-m_1)-\gamma_1 n_c m_1\ , \tag{19}$$

$$\frac{dm_2}{dt}=\lambda_2 h(M_2-m_2)-\gamma_2 n_c m_2\ , \tag{20}$$

$$\frac{dh}{dt}=R-\lambda_1 h(M_1-m_1)-\lambda_2 h(M_2-m_2)\ . \tag{21}$$

Also at all times

$$n_c+n+p=m_1+m_2+h\ . \tag{22}$$

To simplify the problem it was assumed that the concentrations M_1 and M_2 of the available recombination centers were considerably greater than N (values actually used were $M_1=M_2=5N$). This has the effect of essentially combining the four new parameters into two, namely $\lambda_1 M_1$ and $\lambda_2 M_2$.

This program was used to simulate the laboratory γ dosing employed in obtaining the experimental first glow growth curve of Fig. 3. Starting with the initial conditions specified by Eq. (11), final occupation numbers n/N, m_{01}/N, and m_{02}/N were obtained as a function of equally spaced values of dose: D/N. These final occupation numbers were then used as the starting point for calculation of the glow curves using the computer solutions for Eqs. (3)–(7). Since the resulting calculated glow curves increased in width somewhat with dose, while the experimental ones did not, the measure of the TL yield was taken to be the product of H, the peak counting rate, and ω, the FWHM. The parameters were varied until a fit to the experimental first glow growth curve was obtained, producing values of $\lambda_1 N=2.3$ and $\lambda_2 N=0.080$, and calibrating D/N with 0.31 corresponding to 50 Gy. All dose levels were taken to be administered uniformly in a time interval $\Delta=10$ sec, with an additional 10 sec allowed for emptying band charges. Figure 17 shows the results obtained, the open circles are the experimental points, the same as those shown in Fig. 3 and the solid curve is the derived theoretical function. The dashed curve is the saturation exponential fit found in the earlier work[18] also shown in Fig. 3. The two results both fit the data points about equally well.

At an earlier point in the present analysis it was assumed that the saturation of the TL signal with increasing dose could be attributed to the behavior of n/N, resulting in setting $n_0/N=0.33$. The theoretical analysis

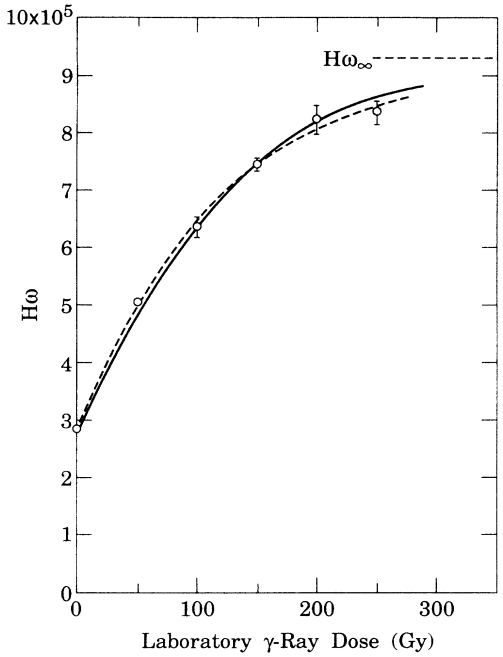

FIG. 17. The growth behavior of green-TL with increasing additive γ-ray dose. The open circles represent the observed data. The units used for TL yield are $H\omega$, peak height H in electrons/s multiplied by the FWHM in °C. The solid curve is the present theoretical fit. The dashed curve is an earlier fit using a least-squares-fitted saturating exponential. The present value for the saturated limit is $H\omega_\infty=9.30\times10^5$.

leading to Fig. 17 indeed shows $(H\omega_0)/(H\omega_\infty)=0.31$ in close agreement, thereby justifying this assumption.

Figure 18 shows the values of m_1/N, m_2/N, n/N, and the value of p/N, which is assumed constant, as functions of the laboratory γ dose. It should be noted that only n/N is actually saturating, i.e., $n/N\rightarrow1.00$. The fact

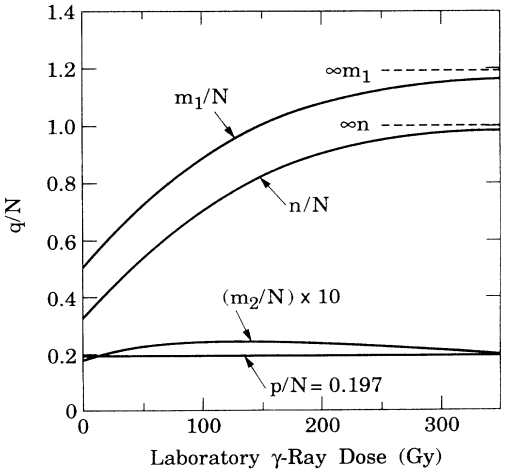

FIG. 18. The behavior of the densities n, m_1, m_2, and p in fractional parts of N as a function of laboratory γ-ray dose. Asymptotic values are $n/N=1.000$, $m_1/N=1.187$, $m_2/N=0.010$, and $p/N=0.197$.

that m_1/N is also approaching a limiting value is a consequence of Eq. (7) for charge conservation. The limiting value of m_1/M_1 is only 0.238, far from saturation. As n approaches N and with p a constant along with the small value of m_2, m_1 is forced to approach a limiting value. The effect might be termed a form of dynamic limiting.

The theory correctly predicts the downward shift in the glow curve peak temperature T_m with increasing dose, but overestimates the magnitude of the shift. For example, the downward peak shift from the natural glow to that for 250 Gy was calculated to be 38 °C rather than the approximately 10 °C observed.

The attempt to use Eqs. (17)–(22) to establish the value of the paleodose from an extrapolation of the additive dose results is confronted with the well-known "midterm fading" problem. The activation energy of the electron trap was found to possess a fairly broad energy distribution. The adopted value of $a=80\ (\text{eV})^{-2}$ yields a FWHM $=0.186$ eV or 12.8% of E_0. Using the time constant $\tau=1/\alpha$ as an indicator for trapped charge decay rates leads to 1.43×10^5 yr at the Gaussian distribution central energy of $E_0=1.45$ eV ($s=5.1\times10^{11}\ \text{sec}^{-1}$ and $T=300$ K), suggesting fairly adequate long term stability for dating purposes. However, for $0.01<\rho(E)<0.5$ of the peak value on the low-energy end of the distribution there results $13.2<\tau<3900$ yr. While these time constants are sufficiently long to validate the previous additive dose calculations they are too short not to produce an age underestimate for samples in the 10^5 yr range. Evidently, a proper paleodose evaluation would require the reintroduction of the activation energy distribution into the charge filling model shown in Fig. 16 and used in the additive dose calculations.

As of this writing the required computer program has not been perfected. Instead a perturbation calculation has been performed, which to first approximation omits the presence of the distribution and then to next order applies a time-dependent decay correction to these results.

Thus, Eqs. (17)–(22) were used to first order in determining the value of the paleodose needed to arrive at the values of n, m_1, m_2, and p given by Eq. (11) representing the state of the natural material. A very long bleaching of this material in our solar simulator reduced the glow peak height of the green-TL emission to a limiting value of about 41% of the unbleached value. A simple model has been developed to explain this type of bleaching of TL yield to a residual value by light to be due to an equilibrium between excitation and de-excitation by the illuminating light (Chen, Hornyak, and Mathur[34]). If, in the present instance, this model is in its essential details applicable, another important feature follows. The equilibrium value of n reached in the last major illumination episode is independent of any past history of ionizing irradiation or light exposure. Thus, a laboratory produced equilibrium value of n may be assumed to be the same value as at the beginning of the paleodose period if the sample were subjected to sufficient sunlight exposure at that time. If in addition, the traps P are assumed saturated throughout the sample history, a reasonable estimate of the initial values at the beginning of the paleodose period may be taken to be

$$\begin{aligned} n_{00}/N&=0.135\ ,\\ p/N&=0.197\ ,\\ m_{001}/N&=0.320\ ,\\ m_{002}/N&=0.012\ . \end{aligned} \tag{23}$$

Using the parameters employed for the additive dose results with these initial values, a dose of $D/N=0.24$ is required by the trap-filling model to arrive at the natural material values given in Eq. (11). To the order of the present approximation this dose translates to 39 Gy and should be compared to a value of 28 Gy arrived at earlier,[18] which assumed that a retrofitted saturating exponential procedure was valid. In addition, the TL-glow yield based on the values given in Eq. (23) was calculated. The resulting value of $H\omega=1.12\times10^5$ is 39% of the natural undosed yield. This value is to be compared to the 41% observed experimentally. The near agreement suggests that the underestimation of the actual dose may indeed be small enough in the present case to be treated as a perturbation.

The time-dependent decay correction, when carried out, results in an underestimation of the paleodose by 11% when the TL is viewed with a green transmission filter. Thus, the true paleodose is 43 Gy. An additional interesting feature of the calculated correction is that had the uv transmission filter been used in these measurements the underestimation of the paleodose would have been about a factor of 2 greater!

A radioactivity assay of the bulk material was made using a direct comparison of γ-ray yields with those of calibrated Bureau of Standards pitchblende-sand and monazite-sand sources. The results were $U=0.70\pm0.03$, $Th=2.00\pm0.22$, and $^{40}K=0.12\pm0.015$ ppm. The sample chemical treatment prior to TL measurements has the consequence of eliminating any α-dose contribution and is estimated to reduce the β-dose contributions to values of $(60\pm15)\%$ for U, $(50\pm20)\%$ for Th, and $(80\pm10)\%$ for ^{40}K relative to maximum doses. The resulting β-dose for all sources yields $(0.155\pm0.026)\times10^{-3}$ Gy/yr; γ-dose for all sources yields $(0.213\pm0.012)\times10^{-3}$ Gy/yr; when these are combined with a cosmic ray dose of 0.120×10^{-3} Gy/yr a total dose of $(0.48_8\pm0.02_8)\times10^{-3}$ Gy/yr is arrived at.

Finally, with a total corrected paleodose of (43 ± 2) Gy the above dose rate gives an age (BPE) $=(88\pm6)\times10^3$ yr. This age should not necessarily be taken to reflect the time of deposition of the sand dunes in this part of the Kalahari desert, although it coincides roughly with the end of the last interglacial, see Nilsson.[35] Since the sample was taken from about two meters below the surface, it

probably represents some sort of time of last excursion by the sample material to the surface, and therefore the time of the last exposure to sunlight. Such churning of materials could, for example, be brought about by a process such as bioturbation.

VI. CONCLUSIONS AND REMARKS

The 375 °C electron trap complex in quartz offers another example demonstrating that the simplest model fit to an experimental glow curve, such as the use of the GOT equation, even if very accurate, need not yield physically correct parameters for the TL process involved. At the very least a simultaneous fit to both a glow curve and an isothermal decay curve must be successfully accomplished before any valid conclusions can be obtained.

In the present instance a large number of experimental results could be fairly well accounted for using a simple interactive kinetic model. This model possesses a single active electron trap coupled to two independent recombination centers by transport through the conduction band. The two centers emit light in different spectral regions, one in the uv and one in the green. Viewed through appropriate optical transmission filters two separate glow peaks appear some 20 °C apart in peak temperature.

The activation energy of the electron trap is of necessity found to possess a fairly broad energy distribution. The adopted value of $a = 80\ (\mathrm{eV})^{-2}$ yields a FWHM equal to 12.8% of E_0 the distribution central energy. The isothermal decay, particularly in its early development, cannot be accounted for without such a distribution. This distribution of activation energies also allows a ready explanation for why the initial rise analysis yields a mean energy considerably lower in value than that actually required in the theory. It may also help to explain why the apparent mean activation energy obtained from a Hoogenstraaten analysis of the dependence of glow curve peak temperatures T_m on heating rate is somewhat higher than the mean activation energy E_0 input to the theory. It is emphasized that the different apparent values of E_0 discussed above are not the result of involving a nonradiative branch depleting the electrons n_c in the conduction band of the type suggested by Wintle, and others.[36–38]

A difficulty that appeared during the course of trying to fit the theory to the data was the simultaneous need for almost first-order kinetic behavior for glow peak shifts with increasing dose and a fairly strong second-order behavior required by the shape characteristics. The problem could be traced to the Gaussian shape assumed for the activation energy distribution, which, while providing a desirable width does not also provide a large enough population of low-energy electrons. This shortage is also evident in the slight difference between theory and experiment in the initial rise portion of the glow curve. Of course, there is no reason to suppose that aside from providing a simple vehicle for the distribution width the Gaussian shape has any validity concerning its detailed features. A distribution shape more of the sort provided by the stretched exponential behavior may be more appropriate.[39]

The model used was kept as simple as possible to test its overall validity. No attempt was made to include "refinements" that, while producing more precise fitting to the data might obscure the main features of the charge trafficking processes involved.[26] Thus, temperature-dependent correction factors such as the $T^{3/2}$ behavior of $\alpha(E)$ resulting from an integration over the momentum phase space in the conduction band were not included.

The model used did not include the possibility of thermal quenching even though the data appeared to suggest the presence of a small decrease in TL yield with increased heating rate. The 375 °C glow peak may well be subject to the same sort of thermal bleaching suggested for the 325 °C glow peak.[36,38,40] As in that case it may be that such bleaching if present is not very marked at the low heating rates used in the present experiments.

Although the isothermal decay in the present model is not an exponential function of time the time constant $\tau = 1/\alpha$ may be used as a rough indicator of decay rates. Applying this consideration to various portions of the activation energy distribution found to fit the present data indicates that for laboratory administered doses at room temperature the entire distribution participates in the processes. However, for paleodose periods in the age range greater than about 5×10^4 yr a supposed equivalent laboratory administered dose will significantly underestimate the age. Also in this age range additive dose curves may not be extrapolated into the paleodose region of doses error free. In the present instance a sample yielding an apparent age of 80 ka had a true paleodose age 11% greater. The same analysis that predicted this age underestimate also attributes different values for the underestimate if the TL data is taken with a uv or green transmission filter; the latter being a considerably smaller correction.

The midterm fading effects described here are reminiscent of such phenomena found elsewhere, for example by Xie and Aitken,[41] although in a completely different context.

It should be noted that the present analysis is for a particular mineralogical sample of quartz. Because of the interactive kinetics involved, the actual paleodose kinetics may be reasonably expected to vary from geological sample to sample as the populations of the recombination centers M_1 and M_2 vary.[40] Finally, determined ages of 10^5 yr and greater without midterm fading corrections may be at serious fault in most cases employing quartz dosimetry.

Note added in proof. In attempting to determine the actual absolute values of β, γ_1, and γ_2, it was found that so long as β/γ_1 and γ_1/γ_2 were kept constant and the condition in Eq. (15b) is not violated, each parameter could be multiplied by a constant and still have the various TL features calculated above remain completely unchanged. Multiplicative constants ranging over three orders of magnitude were tried, always resulting in the same dm_1/dt and dm_2/dt outputs. Thus it is concluded that individual values for β, γ_1, and γ_2 are not obtainable

from the present experimental results. We chose the low values cited for ease of computation.

ACKNOWLEDGMENTS

The authors are indebted to George Hinds for providing a software program to solve the differential equations, Eqs. (17)–(22). We acknowledge the assistance of William Dickerson in taking some of the data. We are also grateful to Mark Gottfried for carrying out numerous calculations. Finally, we wish to acknowledge the support of the National Science Foundation (NSF), Grant No. BNS-9107652.

[1]N. A. Spooner, J. R. Prescott, and J. T. Hutton, Quat. Sci. Rev. **7**, 325 (1988).
[2]A. D. Franklin and W. F. Hornyak, Ancient TL **8**, 29 (1990).
[3]J. R. Prescott and P. J. Fox, Ancient TL **8**, 32 (1990).
[4]A. G. Wintle and D. J. Huntley, Can. J. Earth Sci. **17**, 348 (1980).
[5]A. G. Wintle and D. J. Huntley, Quat. Sci. Rev. **1**, 31 (1982).
[6]D. J. Huntley, Phys. Chem. Minerals **12**, 122 (1985).
[7]A. K. Singhvi and V. Mejdahl, Nucl. Tracks **10**, 137 (1985).
[8]V. Mejdahl, Radiat. Protect. Dosimetry **17**, 219 (1986).
[9]D. J. Huntley, D. I. Godfrey-Smith, and M. L. W. Thewalt, Nature (London) **313**, 105 (1985).
[10]B. W. Smith *et al.*, Radiat. Protect. Dosimetry **17**, 229 (1986).
[11]E. J. Rhodes, Quat. Sci. Rev. **7**, 395 (1988).
[12]M. J. Aitken and B. W. Smith, Quat. Sci. Rev. **7**, 387 (1988).
[13]G. W. S. Wheeler, Quat. Sci. Rev. **7**, 407 (1988).
[14]G. Hütt and J. Jaek, Ancient TL **7**, 48 (1989).
[15]A. S. Brooks *et al.*, Science **248**, 60 (1990).
[16]S. W. S. McKeever, Radiat. Protect. Dosimetry **8**, 81 (1984).
[17]D. J. Huntley *et al.*, J. Lumin. **39**, 123 (1988).
[18]A. F. Franklin, W. F. Hornyak, and W. Dickerson, Quat. Sci. Rev. **11**, 75 (1992).
[19]R. Chen and Y. Kirsh, *Analysis of Thermally Stimulated Processes* (Pergamon, New York, 1981).
[20]G. Bonfiglioli *et al.*, Phys. Rev. **114**, 951 (1959).
[21]W. F. Hornyak and A. Franklin, Nucl. Tracks. Radiat. Meas. **14**, 81 (1988).
[22]G. F. J. Garlick and A. F. Gibson, Proc. Phys. Soc. London, Sect. A **60**, 574 (1948).
[23]A. G. Wintle, Geophys. J. R. Astron. Soc. **41**, 107 (1975).
[24]J. A. Kierstead and P. W. Levy, Proceedings of the 6th International Specialists Seminar (TL) and (ESR) Clermont-Ferrand, 1990 [Nucl. Tracks Rad. Meas. **18**, 19 (1991)].
[25]T. S. C. Singh *et al.*, J. Phys. D **23**, 562 (1990).
[26]A. C. Lewandowski and S. W. S. McKeever, Phys. Rev. B **43**, 8163 (1991).
[27]W. F. Hornyak, P. W. Levy, and J. A. Kierstead, Nucl. Tracks **10**, 557 (1985).
[28]K. W. Wagner, Ann. Phys. (Berlin) **40**, 817 (1913).
[29]W. L. Medlin, Phys. Rev. **123**, 502 (1961).
[30]E. Jahnke and F. Emde, *Tables of Functions* (Dover, New York, 1943).
[31]W. Hoogenstraaten, Philips Res. Rep. **13**, 515 (1958).
[32]W. F. Hornyak and R. Chen, J. Lumin. **44**, 73 (1989).
[33]R. Chen, S. W. S. McKeever, and S. A. Durrani, PACT **6**, 295 (1982).
[34]R. Chen, W. F. Hornyak, and V. K. Mathur. J. Phys. D **23**, 724 (1990).
[35]T. Nilsson, *The Pleistocene* (Reidel, Dordrecht, 1983).
[36]A. G. Wintle, Geophys. J. R. Astron. Soc. **41**, 107 (1975).
[37]A. Delunas *et al.*, J. Lumin. **36**, 373 (1987).
[38]A. G. Wintle, J. Lumin. **33**, 333 (1985).
[39]W. F. Hornyak, R. Chen, and A. Franklin, J. Lumin. **46**, 251 (1990).
[40]M. David *et al.*, Indian J. Pure Appl. Phys. **15**, 201 (1977).
[41]J. Xie and M. J. Aitken, Ancient TL **9**, 21 (1991).